Supporting Information

Erdman *et al*. 10.1073/pnas.0812347106

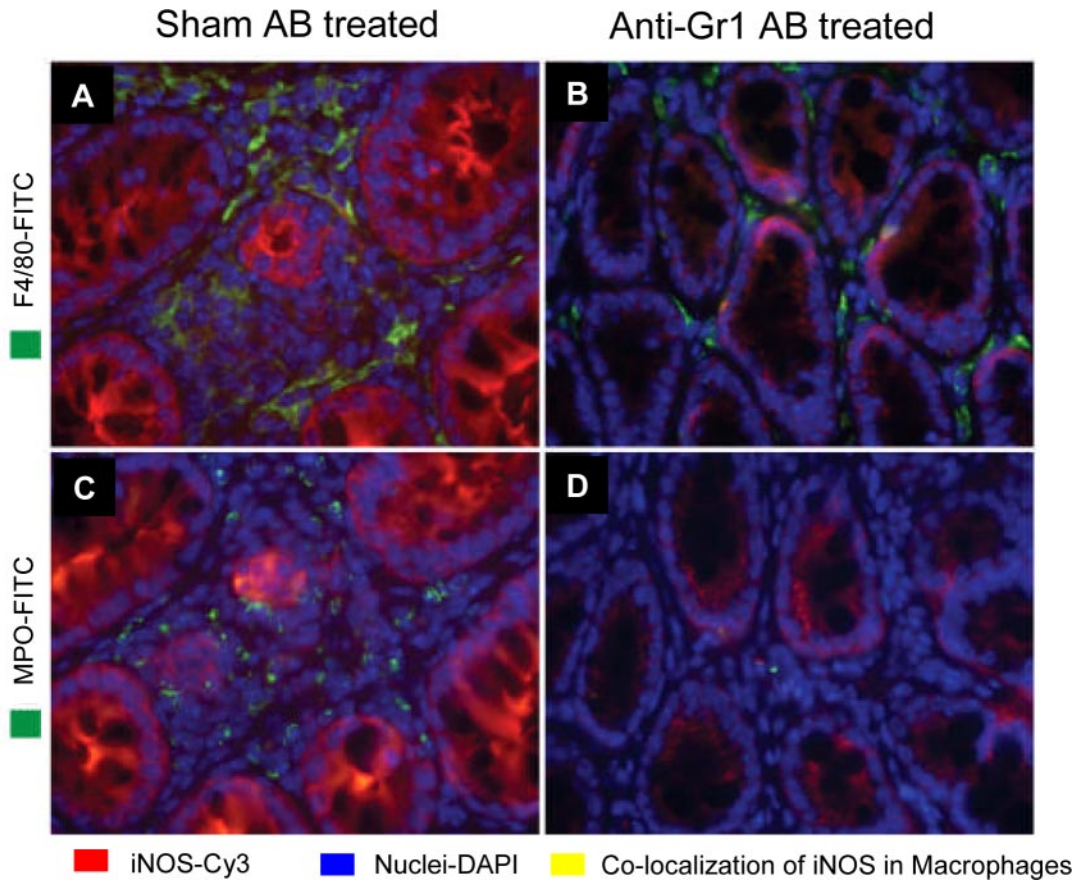

Fig. S1. FIHC revealed that iNOS-expressing F4/80$^+$, MPO$^+$ and epithelial cells observed in the colonic mucosa of sham-antibody-treated *H. hepaticus*-infected Rag 2$^{-/-}$ control mice (*A* and *C*) were significantly reduced after depletion of Gr-1$^+$ cells (*B* and *D*). FITC (green, used for either F4/80$^+$ macrophages or MPO$^+$ cells), Cy3 (red, iNOS) and DAPI (blue, DNA/cell nuclei). (Original magnification, 630×.)

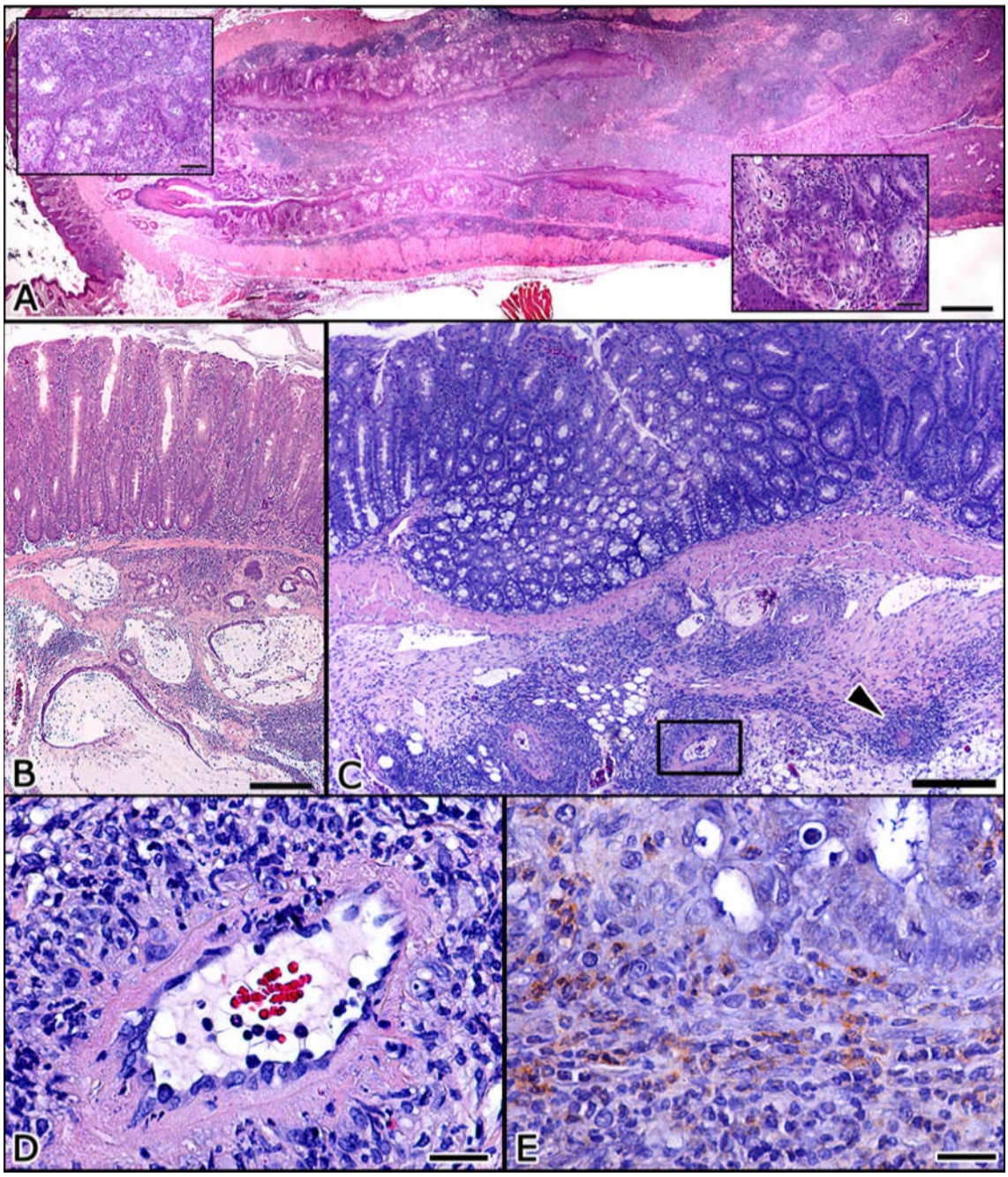

Fig. S2. Pathogenic bacterial infection triggers epithelial dysplasia and carcinoma development in the lower bowel of mice. (*A*) Adenosquamous carcinoma found in a *H. hepaticus*-infected *Rag2*$^{-/-}$ mouse that received T_{EFF} cells at 3 months after infection. The normal architecture of the descending colon, rectum, and anal region is effaced by a prominent squamous neoplastic component admixed with moderately differentiated typical colon adenocarcinoma glands and a dense inflammatory infiltrate. (*Insets*) Histomorphology of squamous differentiation of neoplastic epithelium with inflammatory cells. (*B*) Mucinous adenocarcinoma in the transverse colon was the most common type of colorectal cancer in *H. hepaticus*-infected *Rag2*$^{-/-}$ mice undergoing T_{EFF} cell transfer. Note neoplastic glands and mucin pools partially lined by abnormal epithelium invading into submucosa and muscle layers and obliterating normal architecture. *Helicobacter*-free *Rag2*$^{-/-}$ mice receiving T_{EFF} cells did not develop dysplasia or cancer in the lower bowel (Table 1). (*C*) Characteristic *H. hepaticus*-induced IBD lesions in the ascending colon of an IL10-deficient *Rag2*$^{-/-}$ mouse at 3 months after infection showing mucosal inflammation, hyperplasia, and dysplasia of colonic epithelia. The histopathology of the *H. hepaticus*-infected, IL10-deficient *Rag2*$^{-/-}$ model of IBD differs from the *H. hepaticus*-infected *Rag2*$^{-/-}$ model with increased epithelial hyperplasia and dysplasia in addition to a consistent finding of arteritis nodosa lesions in mice lacking IL10. Arterioles in intestinal serosa, muscularis propria, and mesentery are surrounded by dense inflammatory cell infiltrates. Arrowhead indicates occluded arteriole. (*D*) The arteriole within the boxed area in *C* is shown at a higher magnification. A dense perivascular infiltrate of neutrophils and macrophages effaces the adventitia. Note necrosis of the medial smooth muscle cells with multiple figures of karyorrhexis. (*E*) 7/4-specific immunohistochemistry highlights the increased numbers of neutrophils characterizing *H. hepaticus*-induced colitis in IL10-deficient *Rag2*$^{-/-}$ mice. Hematoxylin and eosin (*A–D*); 3,3-diaminobenzidine, hematoxylin counterstain (*E*). (Scale Bars: 500 μm (*A*); 250 μm (*B* and *C*); 100 μm (*left inset* in *A*); 25 μm (*D* and *E*, *right inset* in *A*.)

Table S1. Pathogenic enteric bacterial infection and inflammatory factors correlate with colonic epithelial dysplasia

Hh	Mutant	Treatment	Colonic inflammation	Colonic dysplasia	Neutrophils 7/4$^+$ cells	Macrophages F4/80$^+$ cells
−	Rag2$^{-/-}$	−	0 (0–0)	0 (0–0)	3.8 ± 0.61	1.2 ± 0.33
+	Rag2$^{-/-}$	−	4 (2–4)	3 (0–4)	28.4 ± 3.33	13.8 ± 1.14
+	Rag2$^{-/-}$	anti-Gr-1	0 (0–3)	0 (0–2)	0.4 ± 0.22	6.6 ± 1.18
+	Rag2$^{-/-}$	anti-TNF	2 (1–2)	0 (0–1)	18.8 ± 2.86	2.8 ± 0.65
+	IL10$^{-/-}$ Rag2$^{-/-}$	−	4 (4–4)	3 (3–4)	45.2 ± 4.56	18.0 ± 2.04
+	WT	−	1 (0–2)	0 (0–0)	8.0 ± 0.87	3.5 ± 0.64

Shown are pathology scores and inflammatory cell counts for select treatment groups. Lesions were graded on a scale of 0−4 with ascending severity. Nonparametric data are presented as median score and range (in parentheses) for each group.

Table S2. Counts of macrophages and neutrophils (per high-power 40× field image)

Infection status	Genotype	Other treatment	Cell counts (mean ± SE)	
			Macrophages ($F4/80^+$)	Neutrophils ($7/4^+$)
−	WT	−	1.4 ± 0.43	3.8 ± 0.74
−	$Rag2^{-/-}$	−	1.2 ± 0.33	3.8 ± 0.61
−	$IL10^{-/-}Rag2^{-/-}$	−	0.9 ± 0.28	4.8 ± 0.47
−	$IL10^{-/-}$	−	12.1 ± 1.23	13.6 ± 1.33
+	WT	−	3.5 ± 0.64	8.0 ± 0.87
+	$Rag2^{-/-}$	−	13.8 ± 1.14	28.4 ± 3.33
+	$IL10^{-/-}Rag2^{-/-}$	−	18.0 ± 2.04	45.2 ± 4.57
+	$IL10^{-/-}$	−	21.4 ± 2.29	13.6 ± 1.33
+	$Rag2^{-/-}$	Sham water	19.9 ± 1.67	42.8 ± 4.76
+	$Rag2^{-/-}$	NMA in water	19.4 ± 0.71	42.9 ± 4.66
+	$Rag2^{-/-}$	wt CD4 + cells	8.4 ± 1.16	8.5 ± 1.58
+	$Rag2^{-/-}$	$IL10^{-/-}$ $CD4^+$ cells	30.4 ± 2.18	31.8 ± 3.59

Cell counts (in situ) of macrophages and neutrophils. Macrophages and neutrophils were identified in intestinal tissue sections with standard avidin-biotin complex (ABC) immunohistochemistry. Rat anti-mouse F4/80 (macrophages) or 7/4 (neutrophils) and biotinylated goat anti-rat IgG (Serotec) were used as primary and secondary antibodies, respectively. Inflammatory cells were quantitated as described in *Materials and Methods*. Cell counts were recorded as the number of macrophages or neutrophils counted per image. The increase of macrophages and neutrophils infiltrating the large bowel mucosa because of infection with *H. hepaticus* was significantly ($P < 0.05$) amplified when infected mice were deficient in lymphocytes or IL10. The adoptive transfer of wild-type CD4-positive lymphocytes down-regulated the frequency of macrophages and neutrophils in the large bowel of Rag2-deficient *H. hepaticus*-infected mice.

Table S3. Pathology scores (cecum)

H. hepaticus			Median score (range) cecum		
Infection status	Genotype	Cell treatment	Inflammation	Hyperplasia	Dysplasia
−	WT	−	0 (0–0)	0 (0–0)	0 (0–0)
−	$Rag2^{-/-}$	−	0 (0–0)	0 (0–0)	0 (0–0)
−	$Rag2^{-/-}$	WT T_{EFF} cells	0.5 (0–1)	0 (0–0)	0 (0–0)
−	$IL10^{-/-}Rag2^{-/-}$	−	1 (0–1)	0 (0–0)	0 (0–0)
+	WT	−	0.5 (0–2)	0 (0–1)	0 (0–0)
+	$Rag2^{-/-}$	−	4 (4–4)	4 (3–4)	3 (1–4) *
+	$Rag2^{-/-}$	WT $CD4^+$ cells	2 (1–3)	0.5 (0–2)	0 (0–2)
+	$Rag2^{-/-}$	WT T_{REG} cells	1 (0–4)	0 (0–3)	0 (0–1)
+	$Rag2^{-/-}$	WT T_{EFF} cells	4 (4–4)	4 (3–4)	4 (3–4) *
+	$Rag2^{-/-}$	WT T_{EFF} + T_{REG} cells	0 (0–1)	0 (0–0)	0 (0–0)
+	$Rag2^{-/-}$	$IL10^{-/-}$ $CD4^+$ cells	4 (4–4)	4 (4–4)	3 (3–4) *
+	$Rag2^{-/-}$	IL10-Ig fusion protein	2.5 (1–4)	1.5 (0–4)	1.5 (0–3)
+	WT	−	0 (0–2)	0 (0–0)	0 (0–0)
+	$IL10^{-/-}$	−	4 (4–4)	4 (4–4)	3.5 (3–4)
+	$IL10^{-/-}Rag2^{-/-}$	−	4 (3–4)	4 (3–4)	3 (2–3)*

Pathology scores of lower bowel for all treatment groups. Formalin-fixed tissues were embedded in paraffin, cut at 5 μm, and stained with hematoxylin and eosin. Lesions were graded on a scale of 0 to 4 with ascending severity as described elsewhere in the text. Nonparametric data are presented as median score and range (in parentheses) for each group. Data were subjected to the Mann–Whitney *U* test for nonparametric data.

*Significance was set at $P < 0.05$. Significant increases in inflammation, hyperplasia, and dysplasia/cancer were observed with deficiency of $Rag2^{-/-}$ and IL10. Significant differences were also observed after *H. hepaticus* infection in $Rag2^{-/-}$ and $Rag2IL10^{-/-}$, and after adoptive transfer of WT T_{EFF} cells. Adoptive transfer of WT T_{REG} cells suppressed inflammation-associated carcinogenesis to baseline levels.